

1 Petrophysical properties of permeable and low-permeable rocks

Reinhard Kirsch

Groundwater conditions at a location are mainly described through the distribution of permeable layers (like sand, gravel, fractured rock) and impermeable or low-permeable layers (like clay, till, solid rock) in the subsurface. To achieve a geophysical image of these underground structures, sufficient contrast of petrophysical properties is required. Seismic velocities (related to elastic properties and density), electrical conductivity, and dielectric constant are the most relevant petrophysical properties for geophysical groundwater exploration.

In this chapter, the influence of porosity, water saturation, and clay content on these petrophysical properties shall be explained.

1.1 Seismic velocities

Seismic velocities for compressional (V_p) and shear waves (V_s) are related to elastic constants like bulk modulus (k), Young's modulus (E), and shear modulus (μ) by

$$V_p = \sqrt{\frac{3k + 4\mu}{3\rho}} = \sqrt{\frac{E \cdot (1 - \nu)}{\rho \cdot (1 + \nu) \cdot (1 - 2\nu)}} \quad (1.1)$$

and

$$V_s = \sqrt{\frac{\mu}{\rho}}$$

with ρ = density and ν = Poisson's ratio.

Since elastic properties of rocks are highly influenced by porosity, e.g. highly porous material is more compressible than material of lower porosity, seismic velocities are also influenced by porosity.

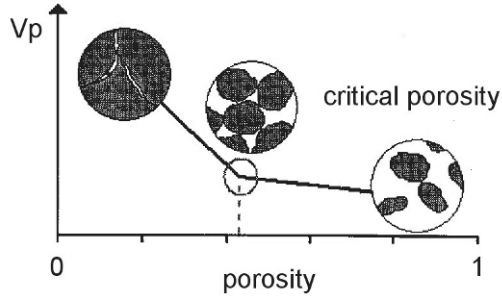


Fig. 1.1. Concept of critical porosity (after Nur et al. 1998)

The following seismic velocity – porosity relations are valid for porosities below the critical porosity threshold (Nur et al. 1998). For porosities above this threshold no grain contacts exist (Fig. 1.1). In that case, mineral grains or rock fragments and pore fluid form a suspension, in which the elastic properties are similar to a fluid. Soil liquefaction associated with earthquakes or landslides are such examples. The critical porosity for most sedimentary rocks is about 40%. As a consequence, seismic velocity – porosity relations are not always valid for structural aquifers formed by tectonic stress.

1.1.1 Consolidated rock

In a simple form, the seismic velocity – porosity relation for consolidated rocks is described by Wyllie et al. (1956) as “time average equation”

$$\frac{1}{V} = \frac{1-\phi}{V_{\text{MATRIX}}} + \frac{\phi}{V_{\text{PORE}}} \quad (1.2)$$

with V_{MATRIX} = seismic velocity of rock matrix or grains
 V_{PORE} = seismic velocity of pore fluid
 ϕ = porosity.

This equation has been modified by Raymer et al. (1980) to:

$$V = (1-\phi)^2 \cdot V_{\text{MATRIX}} + \phi \cdot V_{\text{PORE}} \quad (1.3)$$

A very comprehensive compilation of elastic properties and seismic velocities of porous material is given by Mavko et al. (1998).

A large number of laboratory results on seismic velocities of porous material have been published. Mostly porosity changes were obtained by changes of confining pressure, whereas seismic velocities were measured in the kHz frequency range. Examples of seismic velocity - porosity relations for saturated sandstones found by different authors are (C = volumetric clay content):

$$\text{Han et al. (1986)} \quad V_p = 5.59 - 6.93 \cdot \phi - 2.18 \cdot C$$

$$V_s = 3.57 - 4.91 \cdot \phi - 1.89 \cdot C$$

$$\text{Klimentos (1991)} \quad V_p = 5.87 - 6.33 \cdot \phi - 3.33 \cdot C$$

and for unsaturated sandstone:

$$\text{Kowallis et al. (1984)} \quad V_p = 5.60 - 9.24 \cdot \phi - 5.70 \cdot C \quad [\text{km/s}]$$

Some velocity-porosity relations found by field or laboratory experiments are shown in Fig. 1.2.

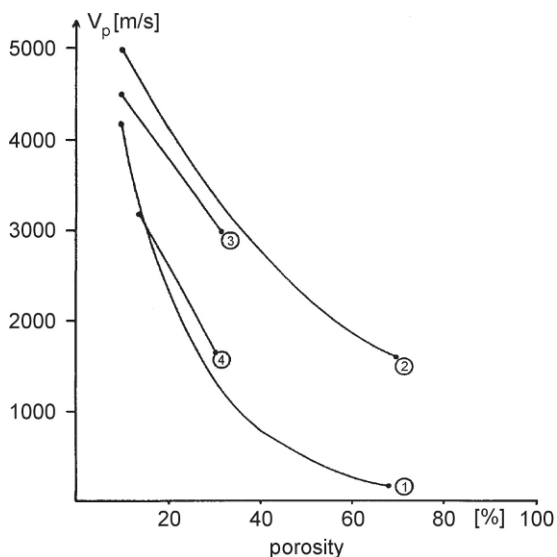


Fig. 1.2. Influence of porosity ϕ on p-wave velocities of sandstone, 1: Watkins et al. (1972), unsaturated rock, refraction seismic measurements, 2: Raymer et al. (1980), saturated rock, model calculations, 3: Klimentos (1991), saturated rock, laboratory measurements, 4: Kowallis et al. (1984), unsaturated rock, laboratory measurements; 1 and 2: clay free material, 3 and 4: clay content $C = 20\%$

1.1.2 Unconsolidated rock

Seismic velocities of unconsolidated rocks (e.g. sand, gravel) are strongly influenced by porosity and water saturation. Fig. 1.3 shows the influence of the water saturation degree on p- and s-wave velocities. No influence of water saturation degree on seismic velocities is observed below a critical value of about 90% water saturation. A further saturation increase leads to a strong increase of p-wave velocity and a slight decrease of s-wave velocity.

Because the shear moduli of air and water are zero, increasing the saturation degree shall have no influence on s-wave velocity. The observed decrease of s-wave velocity can be explained by the increase of density when air is replaced by water as pore filling.

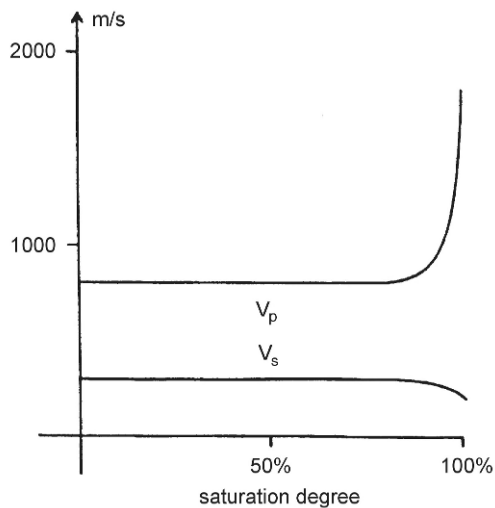


Fig. 1.3. Schematic view on the influence of water saturation on seismic velocities

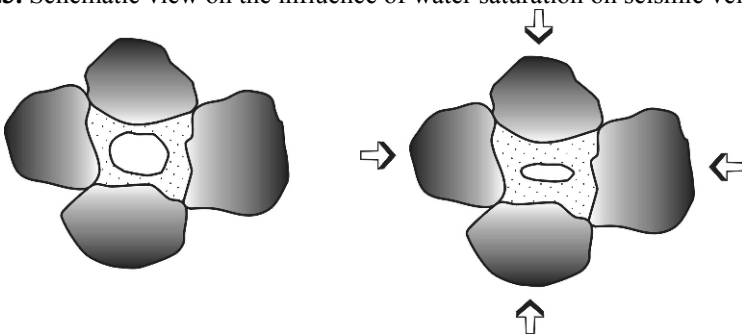


Fig. 1.4. Sketch of a partly saturated pore under compression

The crucial parameter for the p-wave velocity is the bulk modulus related to the compressibility of the material. In Fig. 1.4 a partly saturated pore has been sketched. Pore water is bound by adhesion on the grain surface. If the pore is compressed, the air in the pore space is easily compressible and the pore water cannot increase the bulk modulus of the material. Saturation variations for the partly saturated case below the critical saturation degree have no influence on the bulk modulus and, with the exception of slight density changes, on the p-wave velocity.

Only few field experiments on the influence of porosity on seismic velocities of dry unconsolidated material have been recorded. Watkins et al. (1972) made refraction seismic measurements on outcropping unsaturated hard rock as well as on unsaturated sands and found the following velocity-porosity relation:

$$\phi = -0.175 \cdot \ln(V_p) + 1.56 \quad (1.4)$$

As a consequence, p-wave velocities below sonic velocity (330 m/s) are possible and have been often observed. Bachran et al. (2000) found p-wave velocities as low as 150 m/s for dry beach sands with a velocity-depth increase as shown in Fig. 1.5. This increase can be described by a power law (depth to the power of 1/6). As a consequence, seismic ray paths in the shallow sub-surface are strongly curved.

P-wave velocities for water saturated sands are in the range of 1500 – 2000 m/s (seismic velocity of water: 1500 m/s). Hamilton (1971) measured p-wave velocities of marine sediments which are shown in Fig. 1.6. Morgan (1969) found the following seismic velocity – porosity relation for marine sediments (in km/s):

$$V_p = 1.917 - 0.566 \cdot \phi \quad (1.5)$$

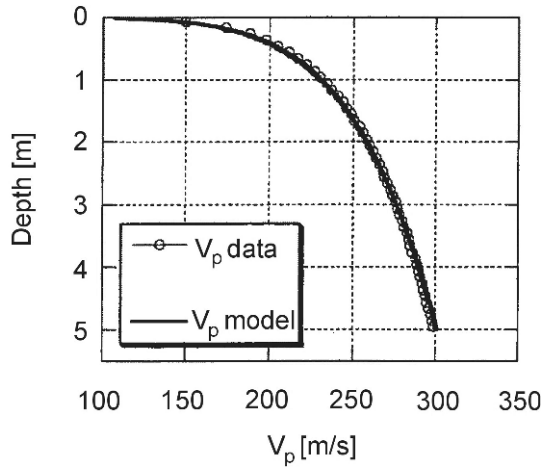


Fig. 1.5. Increase of p-wave velocity with depth (observed and calculated) in the shallow sub-surface (Bachran et al. 2000, with permission from SEG)

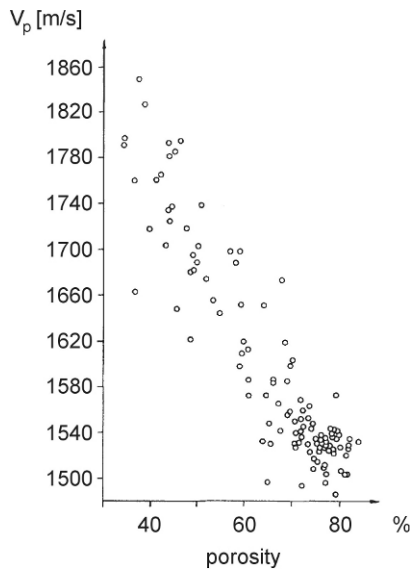


Fig. 1.6. P-wave velocities and porosities for marine sediments (after Hamilton 1971)

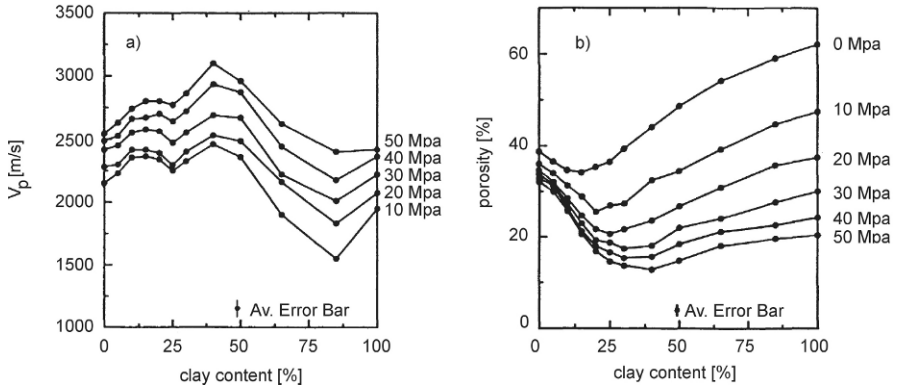


Fig. 1.7. P-wave velocity and porosity for sand-clay mixtures (Marion et al. 1992, with permission from SEG)

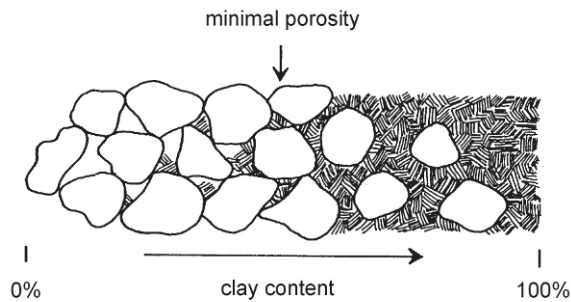


Fig. 1.8. Sketch of sand-clay distribution with increasing clay-content (after Marion et al. 1992)

1.1.3 Clay and till

Clay and till have low hydraulic conductivities. Their hydrogeological importance is that clay or till layers form hydraulic boundaries dividing aquifers.

Till is a mixture of sand, clay, and partly chalk with a wide variety of grain size distributions. The clay content influences the hydraulic conductivity significantly. To investigate the influence of porosity and clay content on seismic velocities, Marion et al. (1992) used artificial sand-clay mixtures for laboratory experiments. A maximum of p-wave velocities was found for clay contents of about 40% (Fig. 1.7).

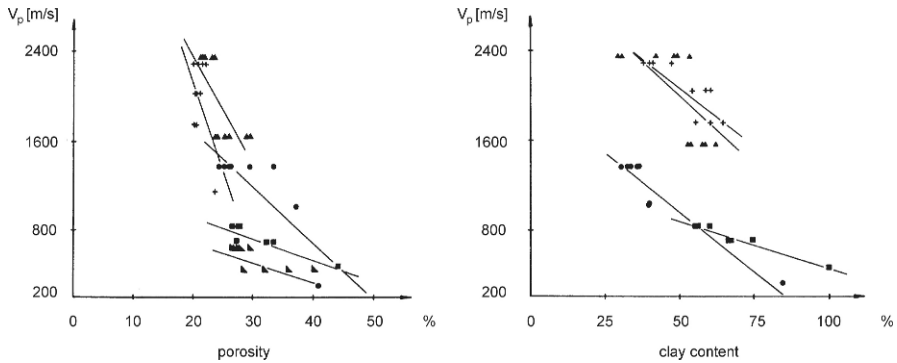


Fig. 1.9. P-wave velocities of tills in relation to porosity and clay content (Baermann and Hübner 1984, with permission from BGR)

An explanation is given in Fig. 1.8. Porosity of clay is about 60%, porosity of sand is about 40%. Small clay content in sands reduce porosity because clay particles fill the pore space. Increasing clay content reduces porosity, until the entire pore space is finally filled with clay. If the clay content is increased further, sand grains loose contact and are isolated in the clay matrix. From that point on, increasing the clay content leads to an increased porosity of the mixture due to the high porosity of clay. It must be taken into account that these results were obtained by using sand and clay of uniform grain size.

Under real field conditions, where tills show a wide variety of grain size distributions, results may not have been so clear. Field measurements on till soils (borehole measurements as well as refraction seismic measurements at steep coasts) by Baermann and Hübner (1984) show decreasing p-wave velocities with increasing porosity and clay content (Fig. 1.9). However, the obtained velocity/porosity or velocity/clay content relations are very site specific and cannot be used in general for an interpretation of seismic velocities.

1.2 Electrical resistivity

1.2.1 Archie's law – conductive pore fluid and resistive rock matrix

Since the electrical resistivity of most minerals is high (exception: clay, metal ores, and graphite), the electrical current flows mainly through the pore water. According to the famous Archie law, the resistivity of water-saturated clay-free material can be described as

$$\rho_{\text{AQUIFER}} = \rho_{\text{WATER}} \cdot F \quad (1.6)$$

ρ_{AQUIFER} = specific resistivity of water saturated sand

ρ_{WATER} = specific resistivity of pore water.

For partly saturated material, F can be replaced by F/S_w^2 (S_w = saturation degree = fraction of water filled pore space).

The formation factor F combines all properties of the material influencing electrical current flow like porosity ϕ , pore shape, and diagenetic cementation.

$$F = a \cdot \phi^{-m} \quad (1.7)$$

Different expressions for the material constant m are used like porosity exponent, shape factor, or (misleading for deposits) cementation degree. Factors influencing m are, e.g., the geometry of pores, the compaction, the mineral composition, and the insulating properties of cementation (Ransom 1984).

The constant a reflects the influence of mineral grains on current flow. If the mineral grains are perfect insulators (main condition for the validity of Archie's law), then $a = 1$. If the mineral grains contribute to the electrical conductivity to a certain degree, the constant a is reduced accordingly.

Typical values for a and m are (after Schön 1996): loose sands, $a = 1.0$, $m = 1.3$, and sandstones, $a = 0.7$, $m = 1.9$. Further examples for a and m are given by Worthington (1993).

Fig. 1.10 shows the influence of the porosity and the porosity exponent m on the formation factor F. For sandy aquifers with porosities ranging from 20 – 30 % formation factors can be expected in the range of 4 - 8. However, as the porosity exponent m is normally unknown, it is difficult to predict the porosity from the measured resistivities of the aquifer, even if the resistivity of the pore water is known. Some values for formation factors in relation to grain size for loose sands are shown in Fig. 1.11.

As the constant m is influenced by pore geometry, the formation factor F is related to tortuosity T. Tortuosity describes how crooked the way of fluid flow through pore space is. Tortuosity depends on porosity, pore shape, and the shape of channels connecting the pores. Assuming that the electrical current flow follows the same path through the pore space as the fluid flow, a relation between formation factor and tortuosity can be found (TNO 1976).

$$F = T \cdot \phi^{-m^*} \quad (1.8)$$

m^* = modified porosity exponent.

A mean tortuosity of $T= 1.26$ was found by TNO (1976) for dune sands and deposits from the river Rhine. Since tortuosity is strongly related to the hydraulic conductivity, Eq. 1.8 gives a link between geophysical and hydraulic properties of the aquifer.

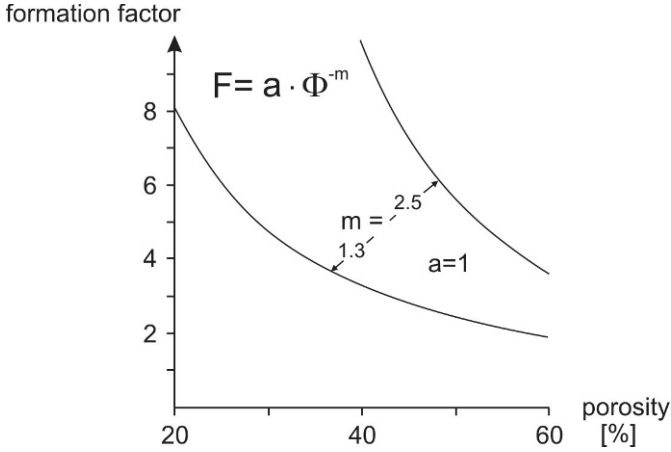


Fig. 1.10. Archie’s law: formation factor F vs. porosity for different porosity exponents

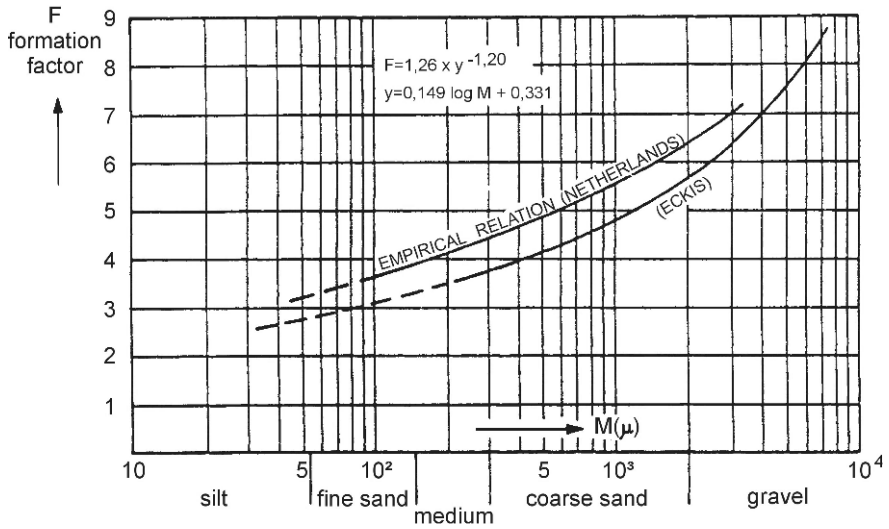


Fig. 1.11. Formation factor dependent on grain size for The Netherlands (TNO 1976, with permission from TNO) compared to results for California (Ecknis 1934), $M(\mu)$ = grain size in micrometer

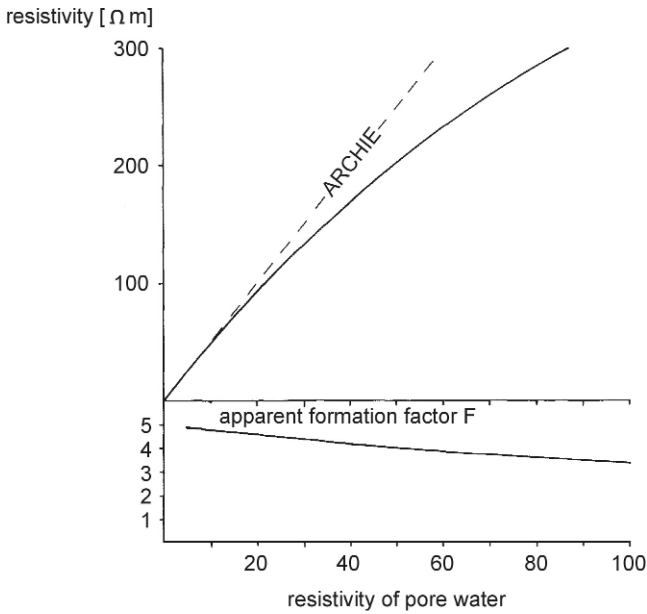


Fig. 1.12. Resistivity and apparent formation factor for high resistive pore water

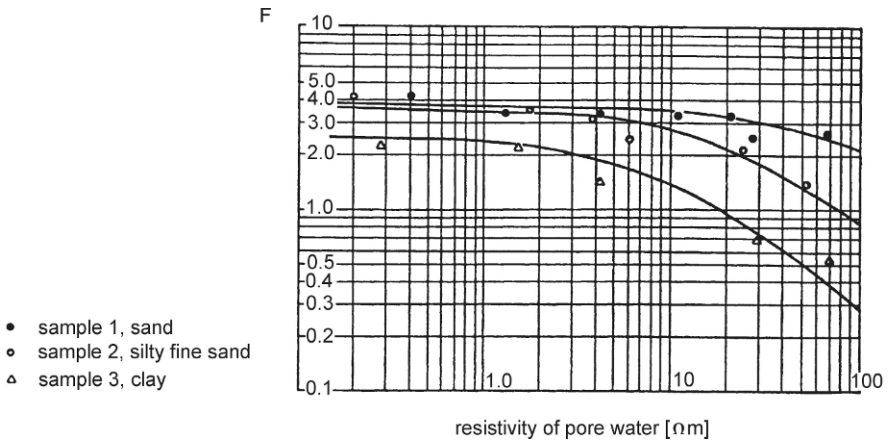


Fig. 1.13. Field examples measured in the Chaco of Paraguay (Repsold 1976, with permission from BGR) for formation factors depending on water resistivity

1.2.2 Limitations of Archie's law – conducting mineral grains

The validity of Archie's law and related formulae is restricted to materials with highly resistive mineral grains and conducting pore fluid. A minor contribution of the mineral grains to electrical conductivity can be taken into account by the constant a . However, when the resistivity of the pore water is sufficiently high that the electrical conductivity of the mineral grains is a substantial contribution to the electrical conductivity of the aquifer, the formulations of Archie are no longer valid. Modified formulations are also required for material with surface conductivity like clay.

High resistive pore water

The electrical resistivity of pore water is controlled by the ion content (salinity) as described in the chapter "Groundwater quality". If the ion content of the groundwater is low resulting in a high bulk resistivity of the aquifer, current flow through the aquifer can be explained by parallel connection of rock matrix and pore fluid (Repsold 1976).

$$\frac{1}{\rho_{\text{AQUIFER}}} = \frac{1}{\rho_{\text{MATRIX}}} + \frac{1}{F \cdot \rho_{\text{WATER}}} \quad (1.9)$$

If we assume a matrix resistivity ρ_{MATRIX} of 1000 Ωm and a formation factor of 5, then even for water resistivity of 20 Ωm aquifer resistivity is clearly lower than expected by Archie's law. If a formation factor is calculated formally by $F = \rho_{\text{AQUIFER}} / \rho_{\text{WATER}}$, a decrease of the so obtained apparent formation factor is observed with increasing water resistivity (Fig. 1.12). Field examples for apparent formation factors depending on water resistivity are shown in Fig. 1.13.

Resistivity of clay and till

Clayey material is characterized by low electrical resistivity in the range of 5 - 60 Ωm and often a target in electrical or electromagnetic surveys. This low resistivity is caused by surface conductivity of clay minerals. As clay minerals are flat, water can diffuse between the minerals and so increase the specific surface area. The specific surface area of clays can be up to 1000 m^2/g , whereas for sands this area is less than 0.1 m^2/g (Scheffer and Schachtschabel 1984). The large specific surface area supports the surface conductivity. Because a number of cations in clay minerals is replaced by cations of higher valence, electrical charge of the clay mineral surface is negative. The negative charge is compensated by the concentration of ca-

tions in the pore water in the vicinity of the mineral surface. This process is quantified by the cation exchange capacity (CEC).

The calculation of the resistivity of clayey material is complicated, since the electrical current flow is possible through clay minerals as well as through pore fluid. A relatively easy approach is given by Frohlich and Parke (1989). They assume that the bulk conductivity of clayey material σ_0 can be explained by parallel connection of surface conductivity σ_{SURFACE} and conductivity of pore water σ_{WATER} with volumetric water content Θ :

$$\sigma_0 = \frac{1}{a} \cdot \sigma_{\text{WATER}} \cdot \Theta^k + \sigma_{\text{SURFACE}} \quad (1.10)$$

or, expressed in terms of resistivity

$$\frac{1}{\rho_0} = \frac{\Theta^k}{a \cdot \rho_{\text{WATER}}} + \frac{1}{\rho_{\text{SURFACE}}} \quad (1.11)$$

The first part of Eqs. 1.10 and 1.11 is related to Archie's law, when exponent k is defined by the saturation degree S_w

$$\Theta^k = S_w^n \cdot \phi^m \quad (1.12)$$

A special case of Eq. 1.10 is given by Mualem and Friedman (1991)

$$\sigma_0 = \sigma_{\text{WATER}} \cdot \frac{\Theta^{2.5}}{\phi} + \sigma_{\text{SURFACE}} \quad (1.13)$$

An expression of surface conductivity (in mS/cm) in terms of volumetric clay content C was found by Rhoades et al. (1989)

$$\sigma_{\text{SURFACE}} = 2.3 \cdot C - 0.021 \quad (1.14)$$

However, for the practical use of Eqs. 1.13 and 1.14, the validity of the empirically determined constants for the project area must be checked.

A more general approach to electrical conductivity of clayey material based on cation exchange capacity is given by Sen et al. (1988):

$$\sigma_0 = \frac{1}{F} \left(\sigma_w + \sigma_w \frac{AQ_v}{\sigma_w + BQ_v} \right) + EQ_v \quad (1.15)$$

Q_v can be expressed by cation exchange capacity CEC, matrix density ρ_{MAT} , and porosity ϕ :

$$Q_v = \frac{\rho_{\text{MAT}}(1-\phi)}{\phi} \text{CEC} \quad (1.16)$$

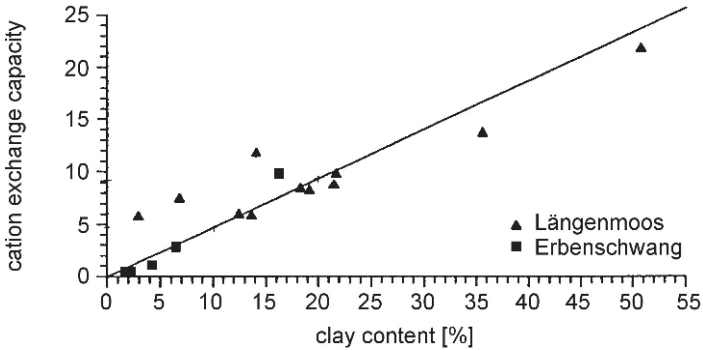


Fig. 1.14. Correlation between clay content and cation exchange capacity for two areas in Southern Germany (Günzel 1994)

According to Günzel (1994), constants A, B, and E are given by $BQ_v=0.7$, $EQ_v=0$, and $A=m\lambda_{na}^S$, with m =porosity exponent of Archie equation and λ_{na}^S = equivalence conductivity of Na^+ -exchange cations, empirically derived as $\lambda_{na}^S=1.94$ (S/m)/(mol/l).

Sen et al. (1988) found an empirical relation between porosity exponent and cation exchange capacity for sandstone samples: $m=1.67+0.2\times CEC^{1/2}$. This can lead to an increase in resistivity with increasing clay content, a clear contradiction to the experience that increasing clay content of unconsolidated material leads to decreasing resistivity. The use of the empirical relation between m and CEC should be restricted to consolidated material. Sen et al. (1988) also mentioned that a good fit of measured data is possible using constant $m=2$.

Eq. 1.15 is valid for saturated material. For partly saturated material, Günzel (1994) replaced Q_v by $Q^*=Q_v/S_w$ (S_w = saturation degree), formation factor F is changed accordingly. Assuming clay free material with $CEC = 0$, Eq. 1.15 reduces to Archie's law $\sigma = \sigma_w/F$.

As shown above, the critical parameter for conductivity of clayey material is not the clay content, but the cation exchange capacity. Cation exchange capacity strictly depends on the mineral composition of clay, which may differ from area to area. Günzel (1994) showed that for smaller areas, where a constant composition of clay minerals can be assumed, a linear relation $CEC = i\times C$ between clay content C and cation exchange capacity exists (Fig. 1.14). As a consequence, if in Eq. 1.16 CEC is replaced by $i\times C$, Eq. 1.15 relates clay content to conductivity.

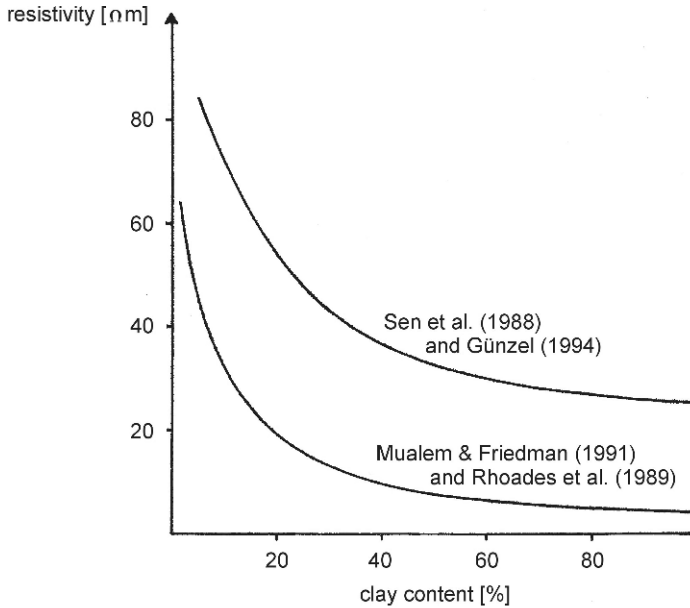


Fig. 1.15. Resistivity of clayey sediments related to clay content by Sen et al. (1988) and Mualem and Friedman (1991). For both relations, porosity of 30% and pore water resistivity of $15 \Omega\text{m}$ were assumed

Using above formulae a comparison between the formalism given by Sen et al. (1988) and the easy formalism of Mualem and Friedman (1991) in Eq. 1.10 is possible. In Eq. 1.10 the surface conductivity σ_s is replaced by Eq. 1.14 (Rhoades et al. 1989), whereas in Eq. 1.16 CEC is replaced by the CEC/clay content ratio found by Günzel (1994) (Fig. 1.14). The results (conductivity converted to resistivity) are shown in Fig. 1.15. Both resistivity-clay content relations show similar shapes, but strong differences for the absolute values. This can be explained by local effects of clay mineral composition in the relations of Günzel (1994) and Rhoades et al. (1989).

Based on the formalism of Sen et al. (1988), an approach to determine clay content from resistivity data is given by Borús (2000). If the lateral distribution of clay content in the near surface subsoil has to be determined by electrical measurements, some reference points with known clay content and resistivity are required in this area. These clay content/resistivity values are displayed in a diagram showing resistivity/clay content curves for different CEC/clay content ratios i (Fig. 1.16). The curve which gives the best fit to the measured data can be used to determine the clay content

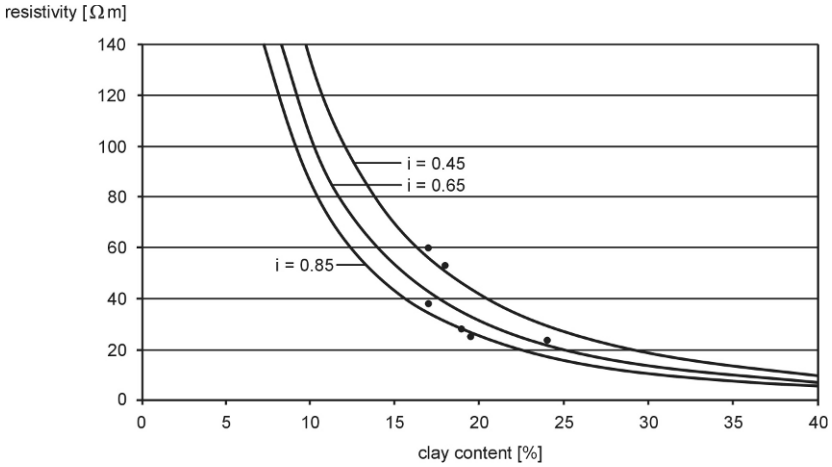


Fig. 1.16. Resistivity-clay content curves for different CEC-clay content ratios *i* after Sen et al (1988). Dots: measured clay content-resistivity values from the Baltic coast area near Kiel. The curve with *i*=0.65 gives the best approached to the measured data and can be used for an assessment of clay content from resistivity values in the project area (Borús 2000)

from the resistivity values measured in the project area apart from the reference points.

1.3 Electric Permittivity (Dielectricity)

Electric permittivity ϵ (more correct: relative permittivity ϵ_r) depends on the polarisation properties of material and is the dominating factor for the propagation speed of electromagnetic waves in the sub-surface which can be calculated from:

$$v = \frac{c}{\sqrt{\epsilon}} \tag{1.17}$$

(*c* = speed of light in vacuum)

The propagation speed of electromagnetic waves is used for time/depth conversion of GPR sections. Because this speed is extremely high, e.g. 3×10^8 m/s in vacuum, normally the "easy to handle" unit cm/ns is used, 3×10^8 m/s then reduces to 30 cm/ns.

Typical values for permittivity ϵ are: water = 80, saturated sand = 20 – 30, and air = 1. High permittivity of water results in strong correlation

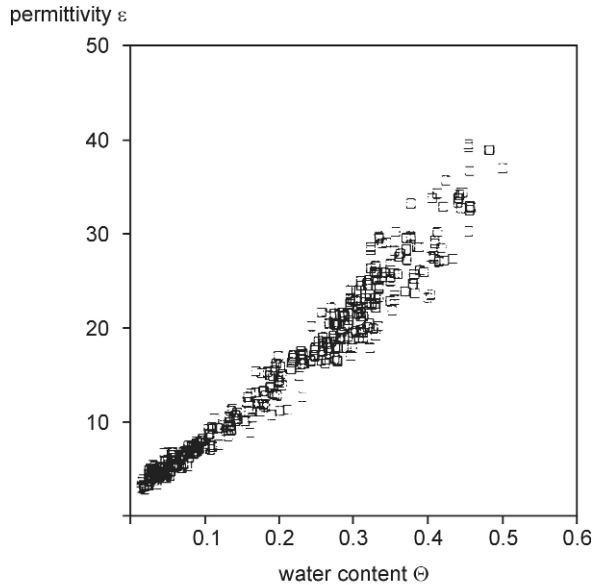


Fig. 1.17. Permittivity of glacial sediments from Finland and Wisconsin (USA) in relation to water content, the data can be fitted by $\epsilon = 3.2 + 35.4 \times \Theta + 101.7 \times \Theta^2 - 63 \times \Theta^3$ (Sutinen 1992, with permission from the Geological Survey of Finland)

between permittivity of material and water content, as shown in Fig. 1.17.

High permittivity of water results from dipole characteristic of water molecules leading to high polarisability. High polarisability is lost when water is frozen. In saltwater, permittivity is also reduced down to $\epsilon = 35$ at total saturation (Kulenkampff 1988). This is caused by electrostatic grouping of dissociated anions and cations around the H^+ and O^{2-} ions of the water molecules reducing polarisability. For GPR measurements, this reduced permittivity and increased propagation speed in saltwater is not important, because due to high absorption of radar pulses in saltwater no sufficient penetration in salty soil can be achieved.

To quantify the influence of porosity ϕ and water content (quantified by the saturation degree S_w on the permittivity ϵ , a general mixing law for a multi-component rock system (Birschak et al. 1974) can be applied:

$$\epsilon^s = \sum_n v_i \cdot \epsilon_i^s \quad (1.18)$$

v_i , ϵ_i volumetric content and permittivity of each component (rock matrix, pore water, etc)

A special case is given by Schön (1996)

$$\epsilon = \phi \cdot S_W \cdot \epsilon_{\text{WATER}} + \phi \cdot (1 - S_W) \cdot \epsilon_{\text{AIR}} + (1 - \phi) \cdot \epsilon_{\text{MATRIX}} \quad (1.19)$$

ϵ_{MATRIX} = permittivity of rock matrix (e.g. quartz grains)
 ϵ_{WATER} = permittivity of water
 ϵ_{AIR} = permittivity of air.

Another special case of the mixing law is the CRIM equation (complex refractive index method) (Schlumberger 1991)

$$\sqrt{\epsilon} = \phi \cdot S_W \sqrt{\epsilon_{\text{WATER}}} + (1 - \phi) \sqrt{\epsilon_{\text{MATRIX}}} + \phi \cdot (1 - S_W) \sqrt{\epsilon_{\text{AIR}}} \quad (1.20)$$

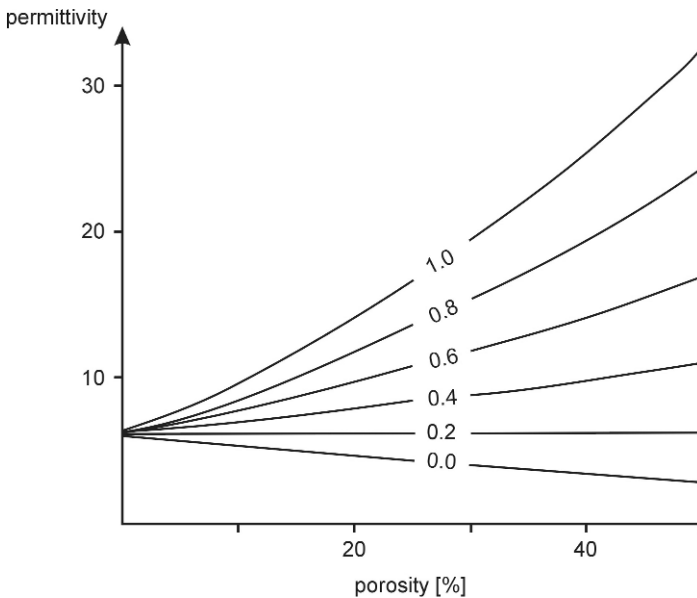


Fig. 1.18. Permittivity vs. porosity and saturation degree after Eq. 1.19

Based on Eq. 1.19 the influence of porosity on permittivity for different saturation degrees is shown in Fig. 1.18. Whereas for saturated pores permittivity increases with increasing porosity, a decrease of permittivity can be expected for air filled pores. For a saturation degree of about 30% which can be assumed for unsaturated sand, no influence of porosity variations on the permittivity can be expected.

A further formalism to calculate the permittivity for partial saturated sediments is the Hanai-Brüggemann mixing law (Graeves et al. 1996). First of all, for the pore filling water/air, an effective permittivity ϵ_{PORE} is calculated:

$$\epsilon_{\text{PORE}} = \epsilon_{\text{WATER}} \cdot S_W^{m_1} \cdot \left(\frac{1 - \frac{\epsilon_{\text{AIR}}}{\epsilon_{\text{WATER}}}}{1 - \frac{\epsilon_{\text{AIR}}}{\epsilon_{\text{PORE}}}} \right)^{m_1} \quad (1.21)$$

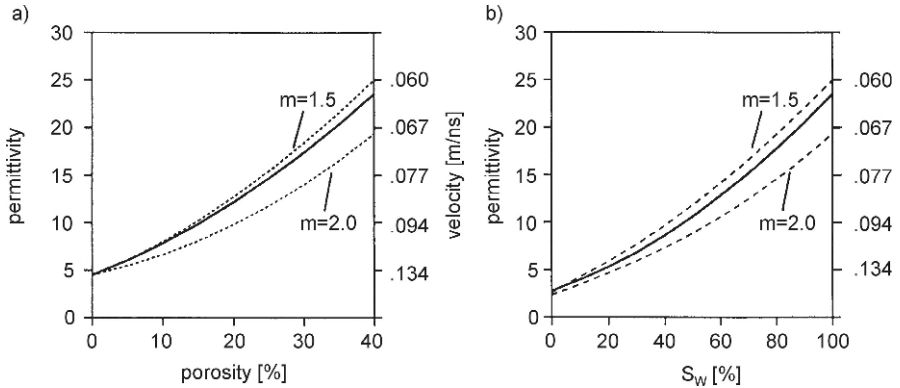


Fig. 1.19. Comparison of CRIM and Hanai-Bruggemann mixing law, a) saturated material, permittivity vs. porosity; b) partly saturated material, porosity 40%, permittivity vs. saturation degree (Graeves et al. 1996, with permission from SEG)

Using an analogue mixing law, the permittivity of partly saturated material can be obtained

$$\epsilon = \epsilon_{\text{PORE}} \cdot \phi^{m_2} \cdot \left(\frac{1 - \frac{\epsilon_{\text{MATRIX}}}{\epsilon_{\text{PORE}}}}{1 - \frac{\epsilon_{\text{MATRIX}}}{\epsilon}} \right)^{m_2} \quad (1.22)$$

Although constants m_1 and m_2 are different, for practical use both can be assumed to be equal (Graeves et al. 1996). A comparison of CRIM and Hanai-Bruggemann mixing law is given in Fig. 1.19. Identical values of 1.5 (unconsolidated sand) and 2 (cemented sandstone) were taken for constants m_1 and m_2 . Assuming a constant $m = 1.6$, both formalisms lead to nearly identical results.

For clayey material with clay content C , the CRIM equation was extended by Wharton et al. (1980)

$$\sqrt{\epsilon} = \phi \cdot S_W \cdot \sqrt{\epsilon_{\text{WATER}}} + (1 - \phi) \cdot (1 - C) \cdot \sqrt{\epsilon_{\text{MATRIX}}} + \phi \cdot (1 - S_W) \sqrt{\epsilon_{\text{AIR}}} + (1 - \phi) \cdot C \cdot \sqrt{\epsilon_{\text{CLAY}}} \quad (1.23)$$

Field values for permittivity of tills were reported by Sutinen (1992) as shown in Fig. 1.20.

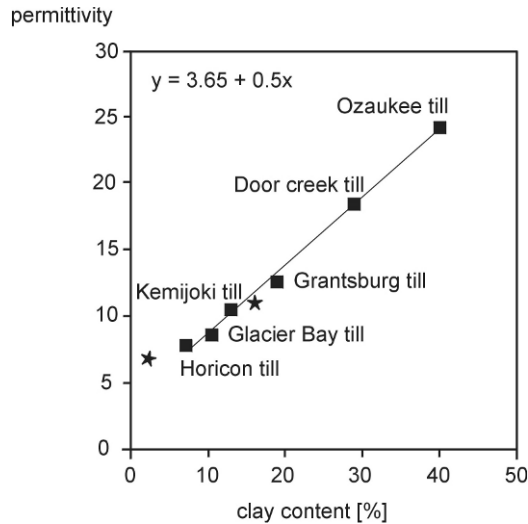


Fig. 1.20. Permittivity of till vs. clay content for samples of Wisconsin (USA), similar results were obtained in other parts of USA (Sutinen 1992, with permission from the Geological Survey of Finland)

1.4 Conclusions

As shown above, in general sufficient contrast of physical properties of saturated and unsaturated material can be expected leading to good conditions for geophysical prospecting. In Table 1.1 typical values for seismic velocities, resistivities, and permittivities for relevant materials are listed.

Resistivity results in the range of 40 – 60 Ωm obtained from Quaternary sediments must be interpreted with care. Following Figs. 1.11 and 1.16 similar specific resistivities are possible for fine grained sand or silt with pore water resistivities below 20 Ωm and for till with low clay content. Both materials have different hydraulic conductivities, so an interpretation of resistivity results in terms of permeable and low permeable layers might be difficult sometimes (see Chap. 14).

	seismics	geoelectrics, electromagnetics		GPR (after Davis and Annan 1989)	
	V_p m/s	resistivity Ωm	conductivity mS/m	permittivity	wave velocity cm/ns (mean)
gravel, sand (dry)	300 – 800	500 – 2000	0.5 – 2	3 - 5	15
gravel, sand (saturated)	1500 – 2000	40 – 200	5 – 17	20 – 30	6
fractured rock	1500 – 3000	60 – 2000	0.5 – 17	20 – 30	6
solid rock	> 3000	> 2000	< 0.5	4 - 6	13
till	1500 – 2200	30 – 60	17 – 34	5 – 40	6
clay	1500 – 2500	10 – 30	34 - 100	5 – 40	6

Table 1.1. Physical properties of permeable and low permeable layers

1.5 References

- Bachran R, Dvorkin J, Nur AM (2000) Seismic velocities and Poisson's ratio of shallow unconsolidated sands. *Geophysics* 65:559-564
- Baermann A, Hübner S (1984) Ingenieurgeologische und geophysikalische Untersuchungen an Geschiebemergeln im Norddeutschen Raum. *Geologisches Jahrbuch C37*:17-57
- Birschak R, Gardener CG, Hipp JE, Victor JM (1974) High dielectric constant microwave probes for sensing soil moisture. *Proc. IEEE*, 62, 93-98
- Borús H (1999) Einsatz geophysikalischer Meßverfahren zur Abschätzung der hydraulischen Durchlässigkeit tonhaltiger Sedimente als Beitrag zum Grundwasserschutz. PhD-Thesis. Christian-Albrechts-Universität Kiel
- Davis, JL and Annan AP (1989) Ground-penetrating radar for high-resolution mapping of soil and rock stratigraphy. *Geophysical Prospecting* 37:531-551
- Ecknis RP (1934) South Coastal Basin Investigation, Geology and Ground Water Storage Capacity of Valley Fill. *State of California Bull.* 45
- Frohlich RK, Parke CD (1989) The electrical resistivity of the vadose zone - field study. *Ground Water* 27:525-530
- Graeves RJ, Lesmes DP, Lee JM, Toksöz MN (1996) Velocity variations and water content estimated from multi-offset ground penetrating radar. *Geophysics* 61:683-695
- Günzel F (1994) Geoelektrische Untersuchung von Grundwasserkontaminationen unter Berücksichtigung von Ton- und Wassergehalt auf die elektrische Leitfähigkeit des Untergrundes. PhD thesis Universität München
- Han DH, Nur A, Morgan D (1986) Effects of porosity and clay content on wave velocities in sandstones. *Geophysics* 51:2093-2107
- Hamilton EL (1971) Elastic properties of marine sediments. *J Geoph Res* 76:579-604
- Klimentos T (1991) The effects of porosity-permeability-clay content on the velocity of compressional waves. *Geophysics* 56:1930-1939

- Kowallis BJ, Jones LEA, Wang HF (1984) Velocity-porosity-clay content systematics of poorly consolidated sandstones. *J Geophys Res* 89:10355-10364
- Kulenkampff J (1988) Untersuchung über die komplexe elektrische Leitfähigkeit von porösen Gesteinen. – Diploma Thesis, Institut für Geophysik, Technische Universität Clausthal
- Marion D, Nur A, Yin H, Han D (1992) Compressional velocity and porosity in sand-clay mixtures. *Geophysics* 57:554-563
- Mavko G, Mukerji T, Dvorkin J (1998) *The rock physics handbook: tools for seismic analysis in porous media*. Cambridge University Press, Cambridge, New York, Melbourne
- Morgan NA (1969) Physical properties of marine sediments as related to seismic velocities. *Geophysics* 34:529-545
- Mualem Y, Friedman SP (1991) Theoretical prediction of electrical conductivity in saturated and unsaturated soil. *Water Resources Research* 27:2771-2777
- Nur A, Mavko G, Dvorkin J, Galmudi D (1998) Critical porosity: A key to relating physical properties to porosity in rocks. *The Leading Edge* 17:357-362
- Raymer LL, Hunt ER, Gardner JS (1980) An improved sonic transmit time - porosity transform. *Trans. SPWLA, 21st Ann Log Symp*:1-13
- Ransom RC (1984) A contribution towards a better understanding of the modified Archie formation resistivity factor relationship. *The Log Analyst*:7-12
- Repsold H (1976) Über das Verhalten des Formationsfaktors in Lockersedimenten bei schwach mineralisierten Porenwässern. *Geologisches Jahrbuch*, E9:19-34
- Rhoades JD, Manteghi NA, Shouse PJ, Alves WJ (1989) Soil electrical conductivity and soil salinity: new formulations and calibrations. *Soil Sci Soc Am J.* 53:433-439
- Scheffer F, Schachtschabel P (1984) *Lehrbuch der Bodenkunde*. Enke Verlag
- Schlumberger (1991) *Log interpretation principles/applications*. Schlumberger Educational Services, Houston
- Schön, JH (1996) *Physical properties of rocks: Fundamentals and Principles of Petrophysics*. Pergamon Press, New York
- Sen PN, Goode PA, Sibbit A (1988) Electrical conduction in clay bearing sandstones at low and high salinities. *J. Appl. Phys.* 63:4832-4840
- Sutinen R (1992) Glacial deposits, their electrical properties and surveying by image interpretation and ground penetrating radar. *Geological Survey of Finland Bulletin* 359, Espoo
- TNO (1976) *Geophysical well logging for geohydrological purposes in unconsolidated formations*. Groundwater Survey TNO, The Netherlands Organisation for Applied Scientific Research, Delft
- Watkins, JS, Walters LA, Godson RH (1972) Dependence of in-situ compressional-wave velocity on porosity in unsaturated rocks. *Geophysics* 37:29-35
- Wharton, RP, Hazen GA, Rau RN, Best DL (1980) *Electromagnetic propagation logging: advances in technique and interpretation*. Soc of Petr Eng, 9267
- Worthington PF (1993) The uses and abuses of the Archie equation, 1: The formation factor-porosity relationship. *Journal of Applied Geophysics* 30:215 – 228
- Wyllie MRJ, Gregory AR & Gardner LW (1956) Elastic wave velocities in heterogeneous and porous media. *Geophysics* 21:41-70